PROCEEDINGS B

royalsocietypublishing.org/journal/rspb

Research

Cite this article: Wakai MK, Nakamura MJ, Sawai S, Hotta K, Oka K. 2021 Two-Round Ca^{2+} transient in papillae by mechanical stimulation induces metamorphosis in the ascidian *Ciona intestinalis* type A. *Proc. R. Soc. B* **288**: 20203207.
https://doi.org/10.1098/rspb.2020.3207

Received: 4 January 2021
Accepted: 21 January 2021

Subject Category:
Development and physiology

Subject Areas:
developmental biology, neuroscience, behaviour

Keywords:
Ca^{2+} signalling, tunicate, Ca^{2+} transient, epithelial conduction, settlement, mechanosensory

Author for correspondence:
Kohji Hotta
e-mail: khotta@bio.keio.ac.jp

Electronic supplementary material is available online at https://doi.org/10.6084/m9.figshare.c.5291807.

THE ROYAL SOCIETY PUBLISHING

Two-Round Ca^{2+} transient in papillae by mechanical stimulation induces metamorphosis in the ascidian *Ciona intestinalis* type A

Maiki K. Wakai[1], Mitsuru J. Nakamura[2], Satoshi Sawai[2], Kohji Hotta[1] and Kotaro Oka[1,3,4]

[1]Department of Biosciences and Informatics, Faculty of Science and Technology, Keio University, Kouhoku-ku, Yokohama 223-8522, Japan
[2]Graduate School of Arts and Sciences, University of Tokyo, Komaba, 153-8902 Tokyo, Japan
[3]Waseda Research Institute for Science and Engineering, Waseda University, 2-2 Wakamatsucho, Shinjuku, Tokyo 162-8480, Japan
[4]Graduate Institute of Medicine, College of Medicine, Kaohsiung Medical University, Kaohsiung City 80708, Taiwan

MKW, 0000-0001-9903-438X; SS, 0000-0003-3764-219X; KH, 0000-0003-4614-7473; KO, 0000-0001-5358-1003

Marine invertebrate larvae are known to begin metamorphosis in response to environmentally derived cues. However, little is known about the relationships between the perception of such cues and internal signalling for metamorphosis. To elucidate the mechanism underlying the initiation of metamorphosis in the ascidian, *Ciona intestinalis* type A (*Ciona robusta*), we artificially induced ascidian metamorphosis and investigated Ca^{2+} dynamics from pre- to post-metamorphosis. Ca^{2+} transients were observed and consisted of two temporally distinct phases with different durations before tail regression which is the early event of metamorphosis. In the first phase, Phase I, the Ca^{2+} transient in the papillae (adhesive organ of the anterior trunk) was coupled with the Ca^{2+} transient in dorsally localized cells and endoderm cells just after mechanical stimulation. The Ca^{2+} transients in Phase I were also observed when applying only short stimulation. In the second phase, Phase II, the Ca^{2+} transient in papillae was observed again and lasted for approximately 5–11 min just after the Ca^{2+} transient in Phase I continued for a few minutes. The impaired papillae by *Foxg*-knockdown failed to induce the second Ca^{2+} transient in Phase II and tail regression. In Phase II, a wave-like Ca^{2+} propagation was also observed across the entire epidermis. Our results indicate that the papillae sense a mechanical cue and two-round Ca^{2+} transients in papillae transmits the internal metamorphic signals to different tissues, which subsequently induces tail regression. Our study will help elucidate the internal mechanism of metamorphosis in marine invertebrate larvae in response to environmental cues.

1. Background

The larvae of marine invertebrates, including crustacea (barnacles), molluscs, ascidians, echinoderms, and Annelida (polychaetes), eventually settle into the substratum and begin metamorphosis [1–5]. In order to initiate metamorphosis, these larvae require specific cues such as simple contact [6], adhesion via an adhesive organ [7–9], temperature, light, and various chemical cues [10,11]. Therefore, it was thought that a specific organ is responsive to external cues and transduces them to internal organs for the subsequent metamorphosis [12–14]. Ca^{2+} signalling is instrumental in the induction of metamorphosis in metazoans [15–19]. However, little is known about how external environmental cues are translated into internal metamorphic signals.

Ascidian papillae form a transient sensory adhesive organ that serves to attach the larva to a substrate, thereby ensuring settlement and the onset of metamorphosis into the filter-feeding adult [20]. After the papillae-mediated adhesion to a substrate, ascidian metamorphosis is characterized by tail regression [7,21].

Papillae seem to permit a larva to assess a substrate's suitability for settlement and metamorphosis. Papillae-mediated larval adhesion is essential for tail regression and tail regression is reportedly abolished in papillae-cut larva [7]. In the larval stage, the ascidian *Ciona* has three papillae. *Foxg* is expressed at the papillae under the ERK pathway [22]. Each papilla contains four glutamatergic neurons [8], which are considered sensory neurons [23,24]. Although papillary sensory neurons have been proposed to have both chemosensory and mechanosensory functions [25,26], there is no direct evidence that papillae can perceive external cues.

We have previously reported the Ca^{2+} dynamics of *Ciona* embryo from gastrulation to the tailbud stages [27], but Ca^{2+} dynamics in later developmental stages have not been reported before. Here, we present direct evidence of mechanical cues to the papillae playing a role in initiating *Ciona* metamorphosis via two-round Ca^{2+} transients.

2. Material and methods

(a) Samples

Ciona adults were obtained from Maizuru Fisheries Research Station (Kyoto University), Misaki Marine Biological Station (University of Tokyo) through the National Bioresource Project (NBRP), and Onagawa Field Center (Tohoku University), Japan. Eggs were collected by dissecting gonoducts. Fertilized eggs were incubated at 18°C until observation. As *Ciona* larvae acquire competence of tail regression after 29.5 h post-fertilization (hpf) [28], we opted to use the stage 29 larvae [29] after 30 hpf.

(b) Preparation of reporter constructs and microinjection and pharmacological treatment

GCaMP6s mRNA was obtained as previously described [27] (see electronic supplementary material).

(c) Fixation of swimming larva and artificial papillae stimulation

The larvae were fixed to a Petri dish coated with poly-D-lysine (PDL) or poly-L-lysine (PLL), referring to practical tips for imaging ascidian embryos [30] (see electronic supplementary material).

(d) Artificial mechanical stimulation of papillae

After establishing the trunk fixation method, we designed a device that consists of a mechanical stimulator, its manipulator, and a holder to apply mechanical stimuli artificially to the papillae of *Ciona* larva. We called this device an 'artificial papillae stimulator' (see electronic supplementary material).

(e) Microscopy

Samples were observed with three different microscopy methods, namely fluorescence microscopy (FM) with a 3CCD camera, confocal laser scanning microscopy (CLSM), and light-sheet microscopy (LSM). For imaging by FM, we followed previous methods [27] (see electronic supplementary material). For LSM, we employed dual inverted selective plane illumination microscopy (diSPIM) with 40 x water immersion lens (NA 0.8, Nikon) mounted on objective piezos with fibre-coupled digital micro-mirror scanners (Applied Scientific Instrumentation, USA) for light-sheet generation. Bidirectional stack images measuring 512 × 512 pixels were acquired by an sCMOS camera (Zyla 4.2, Andor) at a time interval of 7 s using dispim plugin running on ImageJ Micromanager. Images from two directions were registered and fused using MIPAV (NIH) generate fusion plugin.

3. Results

(a) Artificial induction of tail regression by a new experimental system

At first, we verified that the Ca^{2+} indicator GCaMP6 s can sense Ca^{2+} dynamics even at later developmental stages (electronic supplementary material, figure S1, stage 36 [29], late body axis rotation period; see electronic supplementary material). To observe Ca^{2+} dynamics in larva up to the tail regression stage controlling the timing of adhesion, we established a new experimental system for applying artificial mechanical stimulation to the papillae of an individual swimming larva [31]. The larval trunk is immobilized using a PDL-coated glass base to avoid vibration caused by swimming (figure 1*a*). In the absence of stimulation, 94.6% of immobilized larva retained the tail after 29.5 hpf. At this time, *Ciona* larvae can undergo tail regression if they receive adhesive stimulation (figure 1*b*,*c*). By contrast, when the artificial mechanical stimulus was applied to immobilized larvae (figure 1*d*), tail regression was induced in 83% of 12 larvae (figure 1*e*). These results indicate that trunk immobilization prevented tail regression and that our new experimental system can induce tail regression by controlling the timing of mechanical stimulation.

Interestingly, we found that posterior trunk epidermal cells moved towards the posterior at the onset of tail regression (electronic supplementary material, figure S2; Video S1; Video S2; Video S3 from 0:09:41.360), which was the first observable change in the initiation of *Ciona* metamorphosis earlier than the onset of tail regression. Thus, we defined this backward movement of the posterior trunk epidermis as the timing of the start of tail regression, and we could align the time axis for metamorphosis among individuals, thereby linking each developmental stage.

(b) Two-round Ca^{2+} transients in papillae were observed prior to tail regression

To examine Ca^{2+} dynamics during tail regression, we artificially induced tail regression after 29.5 hpf using our new experimental system and observed Ca^{2+} dynamics from early adhesion up until the late body axis rotation period (up to 52 hpf). Hence, prior to artificial mechanical stimulation, in addition to the known Ca^{2+} transient in epidermal cells called CTEC [27], spontaneous Ca^{2+} increases were observed at the posterior sensory vesicle and nerve cord (figure 2*a*, red arrowheads; Video S3, before adhesion), the timing of which coincided partially with larval swimming behaviour, which suggests the excitation of motor neurons. After mechanical stimulation was applied, Ca^{2+} transients were observed in specific tissues (figure 2*b*–*g* and Video S3). Observed transients were composed of two temporally different Ca^{2+} transients

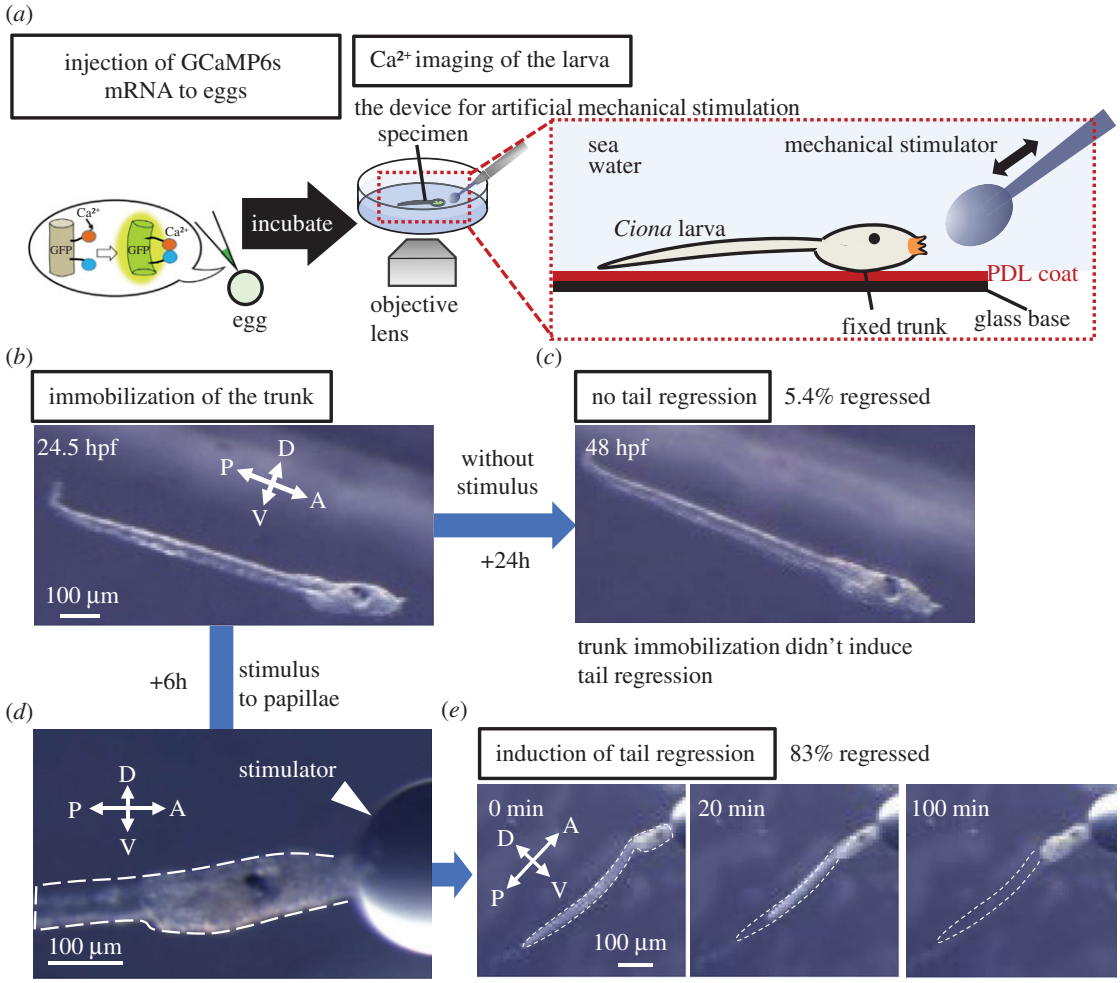

Figure 1. A new experimental system for artificial induction of tail regression. (*a*) A schematic of a new experimental system for observing Ca^{2+} dynamics during artificial induction of tail regression. *GCaMP6s* mRNA, which encodes a Ca^{2+} indicator, was injected into *Ciona* eggs and the injected eggs incubated until observation. PDL-coated (red) dish traps the lateral side of the larval trunk. The papillae can avoid adhesion. Stimuli were applied artificially to the palps using the tip of a glass pole (mechanical stimulator). (*b*) Stereomicroscopic view of a larva immobilized to a PDL-coated dish at 24.5 hpf. (*c*) Stereomicroscopic view of the trapped larva that is not subject to stimulation does not undergo tail regression even at 48 hpf. (*d*) Stereomicroscopic view of a trapped larva subjected to stimulation of the papillae by the mechanical stimulator. The dotted line indicates the larval edge. (*e*) Stereomicroscopic view of a larva subjected to artificial induction of tail regression by mechanical stimulation. Adhesion by the mechanical stimulator started at time 0. At 20 min, the tail tip started to shrink. The tail retracted up to the trunk at 100 min. The dotted line indicates the larval tail edge before tail regression. Abbreviations: A, anterior; D, dorsal; P, posterior; V, ventral. Scale bar: 100 µm. (Online version in colour.)

(figure 2*h*). In the first phase, Phase I, a relatively short-range Ca^{2+} transient was observed immediately after mechanical stimulation. Subsequently the second phase, called Phase II, includes the Ca^{2+} transients observed within 10 min after Phase I.

Phase I was observed immediately after mechanical stimulation and lasted an average of 1.3 min in papillae (figure 2*a–e* and *i*; electronic supplementary material, table S1). The Ca^{2+} transient in Phase I showed fluctuation which suggests that Ca^{2+} transient consisted of the accumulation of multiple Ca^{2+} spikes (figure 2*i*). During Phase I, the Ca^{2+} transient was first observed at both the papillae (figure 2*b*, orange arrowhead) and the dorsal subregion in the posterior trunk (figure 2*b*, white arrowhead; electronic supplementary material, Video S3, time point = 0:01:00). Immediately after the Ca^{2+} transient in the dorsal subregion, the propagation to the ventral region was observed to the endodermal subregion (figure 2*c*,*d*, blue arrowheads; Video S3, time point = 0:01:06). Interestingly, the Ca^{2+} transient in two areas, the papillae and the endoderm, is temporally different but frequently observed to be coupled (figure 2*b–d* and *i*). The Ca^{2+} transient in the papillae reached its maximum intensity an average of 3.6 s earlier than in the endodermal region.

After Phase I, Phase II including the second Ca^{2+} transient in papillae without coupling with the endoderm was observed. The second Ca^{2+} transient reached a peak at 3.2 ± 1.0 min after the maximum peak of the first Ca^{2+} transient (electronic supplementary material, table S1, c). It took 5.3 ± 0.8 min from the peak to stable state (electronic supplementary material, table S1, d). After 8.9 ± 3.3 min lasting of the second Ca^{2+} transient, larvae started tail regression (electronic supplementary material, table S1, f). During Phase II, various tissues, including the epidermis and epidermal sensory neurons, as well as CNS, endoderm, and papillae, exhibited increased Ca^{2+} activity (see electronic supplementary material, Video S3). In particular, wave-like propagations by strong Ca^{2+} increases were observed at whole epidermal cells ($n = 6/6$, figure 2*f*; see electronic supplementary material, Video S3, time point 0:03:17–0:06:21) before tail regression. Compared with before tail regression, the Ca^{2+} activity of the extraembryonic region located in the larval tunic, including motile test cells and extracellular ciliated structure, ASNET [32,33], increased.

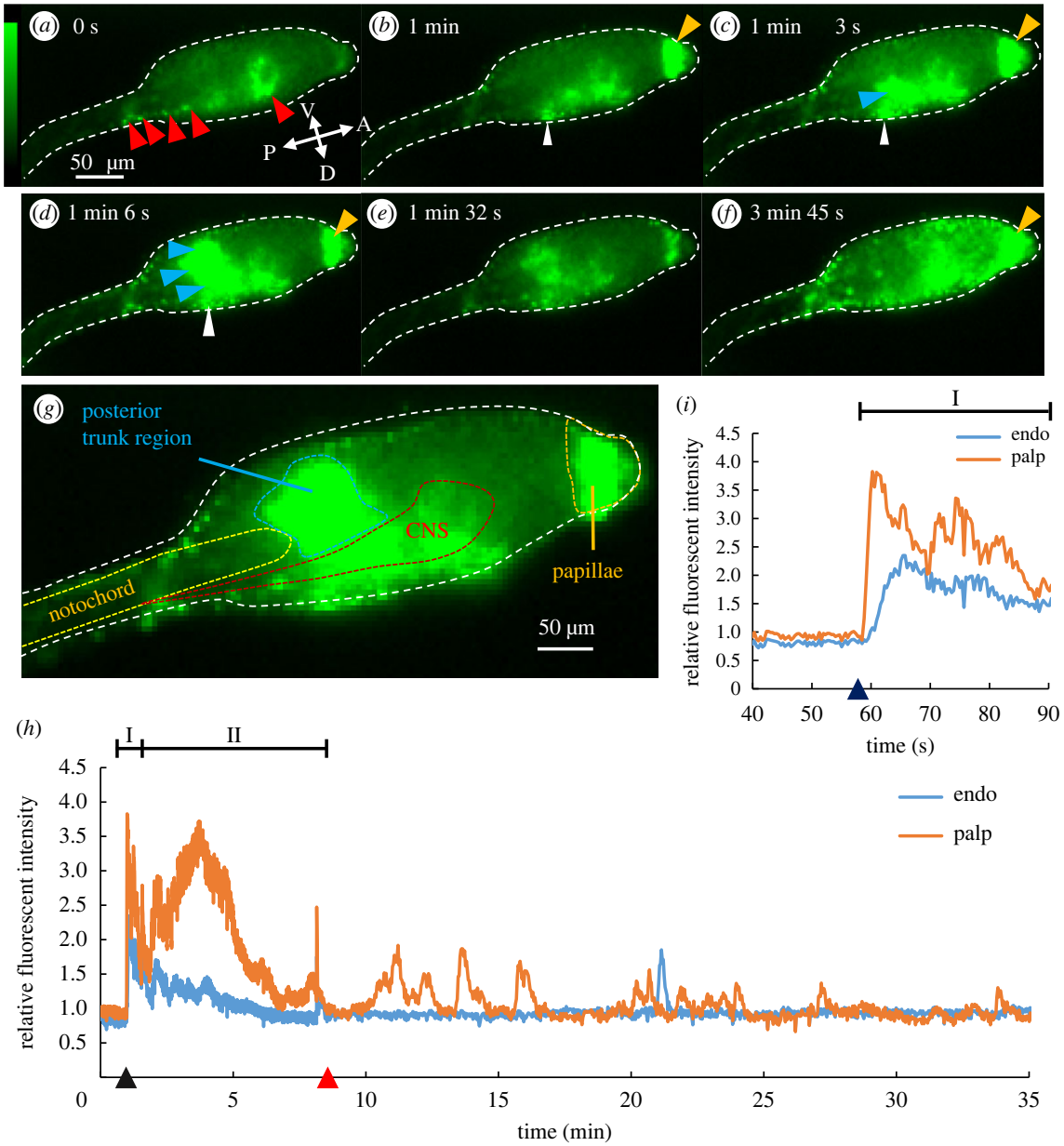

Figure 2. Two-round Ca^{2+} transients observed before the initiation of tail regression. (*a–f*) Ca^{2+} dynamics observed by FM in *Ciona* from the larval period to adhesion period. The white dotted line indicates the larval edge. (*a*) Spontaneous Ca^{2+} increase in the central nervous system (CNS) (red arrowheads). (*b*) The larva at 1 min after mechanical stimulation was applied. Ca^{2+} increase was observed in the palps (orange arrowhead) and the dorsal cells in the posterior trunk (white arrowhead). (*c*) Ca^{2+} increase in part of the dorsal posterior endodermal region (blue arrowhead) in addition to the palps and the dorsal cells (white arrowhead). (*d*) The Ca^{2+} increase in dorsal posterior endodermal region observed in (*c*) propagated to ventral side (blue arrowheads). (*e*) The Ca^{2+} increase in both the palps and trunk decreased with time. (*f*) The Ca^{2+} increase in the palps again as well as across the entire epidermal region. (*g*) Anatomical information of the anterior region of larva superimposed with the Ca^{2+} image by FM. Observed regions were subdivided into CNS (red), papillae (orange), notochord (yellow), and posterior trunk region corresponding to endoderm (blue). (*h*) The relative fluorescence intensity of papillae (orange) and endoderm (blue). In Phase I, a short Ca^{2+} transient was observed in both the papillae and endoderm (I) following adhesion (dark blue triangle). In Phase II (II), Ca^{2+} transient in palps was observed before tail regression (red triangle). (*i*) Enlarged graph of Phase I in (*h*). After adhesion, the Ca^{2+} transient in the palps was accompanied by the Ca^{2+} transient in the trunk region. Abbreviations: A, anterior; D, dorsal; P, posterior; V, ventral. Scale bar: 50 µm. (Online version in colour.)

As two-round Ca^{2+} transients (Phase I and Phase II) at the papillae were observed in all tail-regressed larvae (table 1), Phase I and Phase II appear to be involved in inducing *Ciona* tail regression.

(c) The Ca^{2+} transient in Phase I responding to the mechanical stimulation

Phase I starts immediately after adhesion (figure 2*h*). In addition, the anatomical investigation has suggested that ascidian papillae sense mechanical stimulation [8,25,33–36]. These two results suggest that the papillae sense a mechanical stimulus and the Ca^{2+} transient in Phase I is in response to papillary mechanical stimulation. To understand the detailed profile of Phases I and II in tail regression, we first determined the relationship between the mechanical cue and induction of Phase I. Mechanical stimulation of different durations (2, 5, and 13 s) were applied to the larval papillae after 26.5 hpf (figure 3*a*) and Ca^{2+} responses were recorded. The Ca^{2+} transient in papillae and trunk region was observed in a similar manner to the Ca^{2+} transient in Phase I (electronic supplementary material, table S2) for all stimuli. The Ca^{2+} transient in

Table 1. The number of samples showing Phase I, Phase II and tail regression after different lengths of mechanical stimuli. From the left-hand column, the duration of mechanical stimulation was 0 s, 10 s, and continuous.

	stimulus			
	0 s	10 s	continuous	
	ctrl			*Foxg* MO
Phase I	0/8	3/3	6/6	4/13
Phase II	0/8	0/3	6/6	0/13
tail regression	0/8	0/3	6/6	3/13

papillae was followed by the trunk region (figure 3*b*, blue arrowheads; electronic supplementary material, table S2) occurring 1.95 s later, as suggested by cross-correlation analysis (figure 3*c*; electronic supplementary material figure S4; Video S4; electronic supplementary material, table S3). Regardless of the length of mechanical stimulation, the trend of Ca^{2+} transients (figure 3*c*) was similar to the trend of Ca^{2+} transient during Phase I (figure 2*i*, electronic supplementary material, figure S5).

Based on these results, we concluded that papillae sensed mechanical stimulation and the Ca^{2+} transient in Phase I is triggered by the mechanical stimulation of the papillae and Ca^{2+} transient in the posterior trunk region coupled with that of the papillae. Consistent with this conclusion is the observation that swimming larvae did not show Phase I without adhering to the substrate (figure 4*a*) while all individuals that experienced tail regression experienced Phase I (figure 2*h*; electronic supplementary material, figure S3A–E).

(d) The Ca^{2+} transient in Phase II coupled with tail regression

Next, we characterized Phase II, where a relatively long-lasting second Ca^{2+} transient was observed after Phase I. Because Phase II was just before tail regression (figure 2*h*; electronic supplementary material, Video S3) and larvae require continuous adhesion for at least 28 min to start tail regression [28], Phase II was assumed to comprise Ca^{2+} transients that arise during the continuous adhesion required to initiate tail regression. In order to demonstrate the necessity of the second Ca^{2+} transient in papillae to start tail regression, we verified two requirements. The first requirement is that the second Ca^{2+} transient happens specifically before tail regression while the second is that the second Ca^{2+} transient never happens in response to brief stimulation because only continuous adhesion can induce tail regression.

First, we investigated whether the second Ca^{2+} transient occurs only before tail regression. We compared Ca^{2+} dynamics between no stimulation and continuous adhesion in larvae after 29.5 hpf (figure 4*a*,*c*). The second Ca^{2+} transient did not occur in the absence of stimulation (figure 4*a* and table 1, column of 0 s). By contrast, all larvae that underwent metamorphosis displayed the second Ca^{2+} transient (figure 4*c* and table 1, column of continuous). Phase II occurred only when tail regression was observed. We therefore propose that the second Ca^{2+} transient of papillae is essential for tail regression.

Second, to determine if the second Ca^{2+} transient specifically occurs when the larva is stimulated for a sufficiently long duration to induce tail regression, we applied 10 s of continuous stimulation after 29.5 hpf (figure 4*b*,*c*). Following brief stimulation, the Ca^{2+} transients in Phase I was observed but the Ca^{2+} transient in Phase II and tail regression did not occur (figure 4*b* and table 1, column for 10 s stimulus). By contrast, all larvae subject to longer stimulation metamorphosed and showed Ca^{2+} transient in both Phase I and Phase II (figure 4*c* and table 1 ($n = 6$)). Since the second Ca^{2+} transient was observed only when continuous stimulation was applied, continuous stimulation (12 min average from adhesion to start of tail regression in this study) appears to induce the second Ca^{2+} transient. Moreover, only larvae that showed the second Ca^{2+} transient began tail regression (table 1) suggesting that the second Ca^{2+} transient induces tail regression. These results suggest that Ca^{2+} transients in Phase II are essential for the start of tail regression.

In addition, to clarify how the papillae differentiation is associated with the induction of Ca^{2+} transient in Phase I and Phase II and subsequent tail regression, we examined the dynamics of Ca^{2+} transient and tail regression in *Foxg*-knockdown larva. It has been reported that *Foxg* is expressed in larval papillae where it functions to specify the papillae as sensory neurons [22]. During embryogenesis, *Foxg* expression in neural plate cells is controlled by the mitogen-activated protein kinase (MAPK)/ERK. In *Foxg*-knockdown larva, short Ca^{2+} transients were observed at the anterior trunk epidermis under continuous stimulation. However, neither the second Ca^{2+} transient in Phase II nor tail regression was observed (figure 4*d* and table 1). This result suggests that *Foxg*-specified sensory neurons are required for the generation of the second Ca^{2+} transient and tail regression.

(e) Identification of tissues observed during the first round of Ca^{2+} transients

Finally, we identified precise anatomical regions where Ca^{2+} activity increased during Phase I. In Phase I, the Ca^{2+} transient was first observed at both the papillae (figure 2 and figure 5, orange) and the dorsal subregion in the posterior trunk (figure 2 and figure 5, white arrowhead), before the Ca^{2+} increase in the dorsal subregion propagated to the ventral endodermal region (figure 2 and figure 5, blue).

Comparing these locations with our phalloidin staining results (figure 5*b*), the Ca^{2+} transient in the papillae include the more posterior part called the preoral lobe (figure 5*b*, orange). The dorsal subregion corresponded to cells located dorsally above the neck region of the central nervous system and the epidermal region (figure 5*b*, white arrowheads) [23,32,33,37]. The Ca^{2+} transient in the endodermal region (figure 2) was identified as endoderm surrounding the anterior tip of the notochord (figure 5*b*, blue). Because this is the first report of a Ca^{2+} transient being observed in the endoderm at the beginning of metamorphosis, we focused on the region expressing the Ca^{2+} transient in response to the mechanical cue. To derive more anatomical information about this region, we performed *in vivo* Ca^{2+} imaging using LSM. Consistent with our phalloidin staining results, a simultaneous Ca^{2+} transient was observed in both the papillae and the endodermal cells contacting the anterior part of the notochord

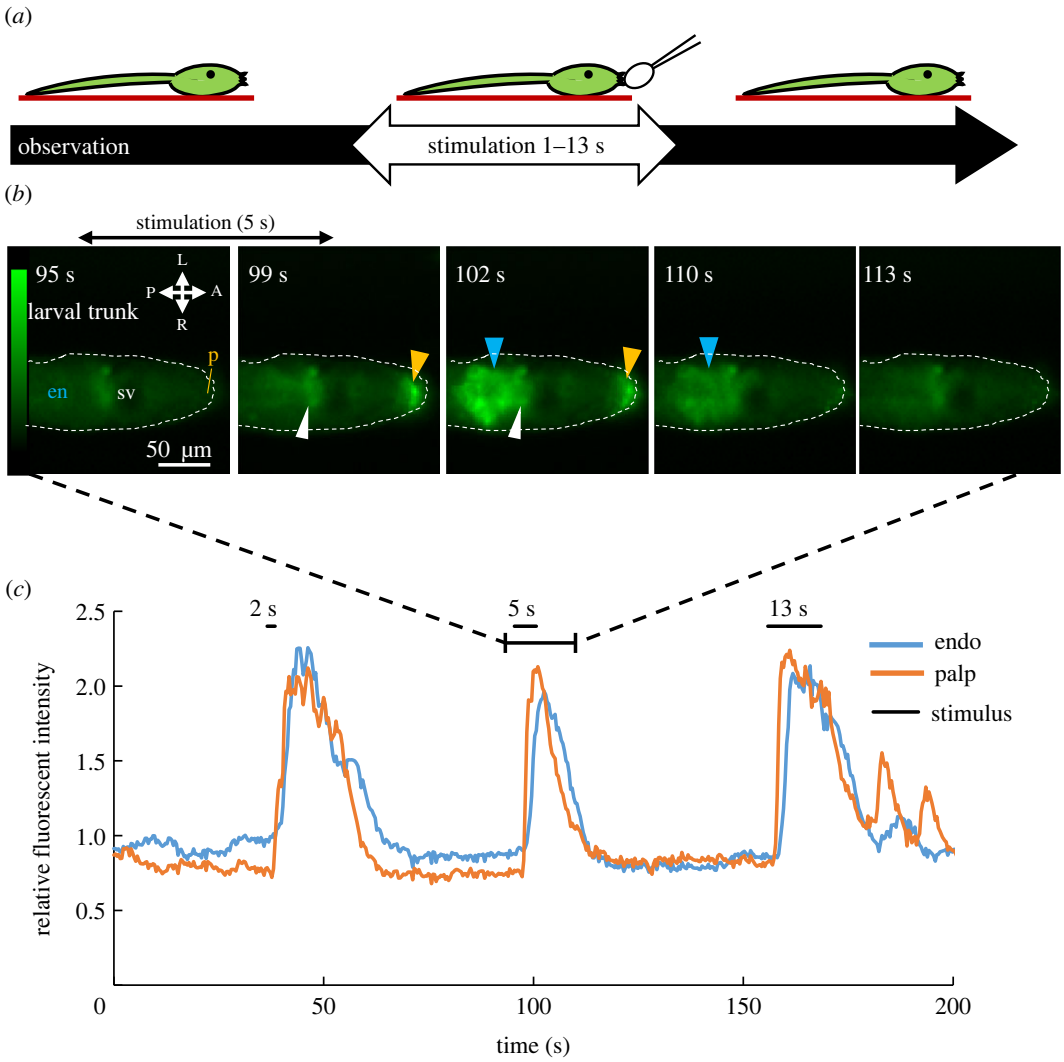

Figure 3. Ca^{2+} transient in Phase I responding to mechanical stimuli. (*a*) Schematic of the experiment. Larva immobilized to PDL-coated dish (red line) was stimulated mechanically for 2, 5, and 13 s. (*b*) Ca^{2+} dynamics of the *Ciona* trunk region during mechanical stimulation observed by FM. For example, a 5 s mechanical stimulus was applied between the 96 and 101 s time points. The Ca^{2+} transient in palps (orange arrowhead) was coupled to the Ca^{2+} transient of the dorsally localized cells (white arrowhead) and the trunk endodermal region (blue arrowhead). Abbreviations: en, endoderm; sv, sensory vesicle. (*c*) The relative fluorescence intensity in the palps and trunk responding to various lengths of mechanical stimulation for 2, 5, and 13 s. Black bars indicate the stimulation period. (Online version in colour.)

(figure 5*a–d*; electronic supplementary material, Video S5). This region was identified as the future digestive tract, in agreement with a previous study that identified the same region as the future digestive tract [38]. These results indicate that the papillary Ca^{2+} transient was coupled with that of the dorsally localized cells in the posterior trunk and the primordial digestive tract in Phase I.

4. Discussion

How larvae perceive environmental cues, such as mechanical stimuli, chemical ligands, temperature, and light, before triggering metamorphosis had evaded researchers until now.

In this study, we revealed novel insights about the role of Ca^{2+} transients in ascidian to link external cues to inner signals that control metamorphosis through precise timing and targeting of specific tissues.

We have identified a two-round Ca^{2+} transient in the adhesive papillae that respond to mechanical cues to initiate metamorphosis in *Ciona* larvae. The observed Ca^{2+} transients resulting from mechanical stimulation up until tail regression (electronic supplementary material, Video S3) are summarized as follows (figure 6).

Phase I)

(1) Ca^{2+} transient in papillae in response to mechanical stimulation (figure 3)
(2) Ca^{2+} transient in dorsally localized cells after (1) (figure 5)
(3) Ca^{2+} transient in dorsal endoderm near the dorsally localized cells (figure 2*c*)
(4) Ca^{2+} propagation from the dorsal endoderm (3) to the ventral endoderm (figure 2*d*)

Phase II)

(5) 2nd-round Ca^{2+} transient in the papillae (figure 2*h*; electronic supplementary material, figure S3)
(6) Ca^{2+} increase in cells across the entire epidermis with wave-like propagation (figure 2*f*; electronic supplementary material, Video S3)
(7) Backward movement of posterior trunk epidermis (figure 1; electronic supplementary material, figure S2, Video S1, S2 and S3)
(8) Tail regression

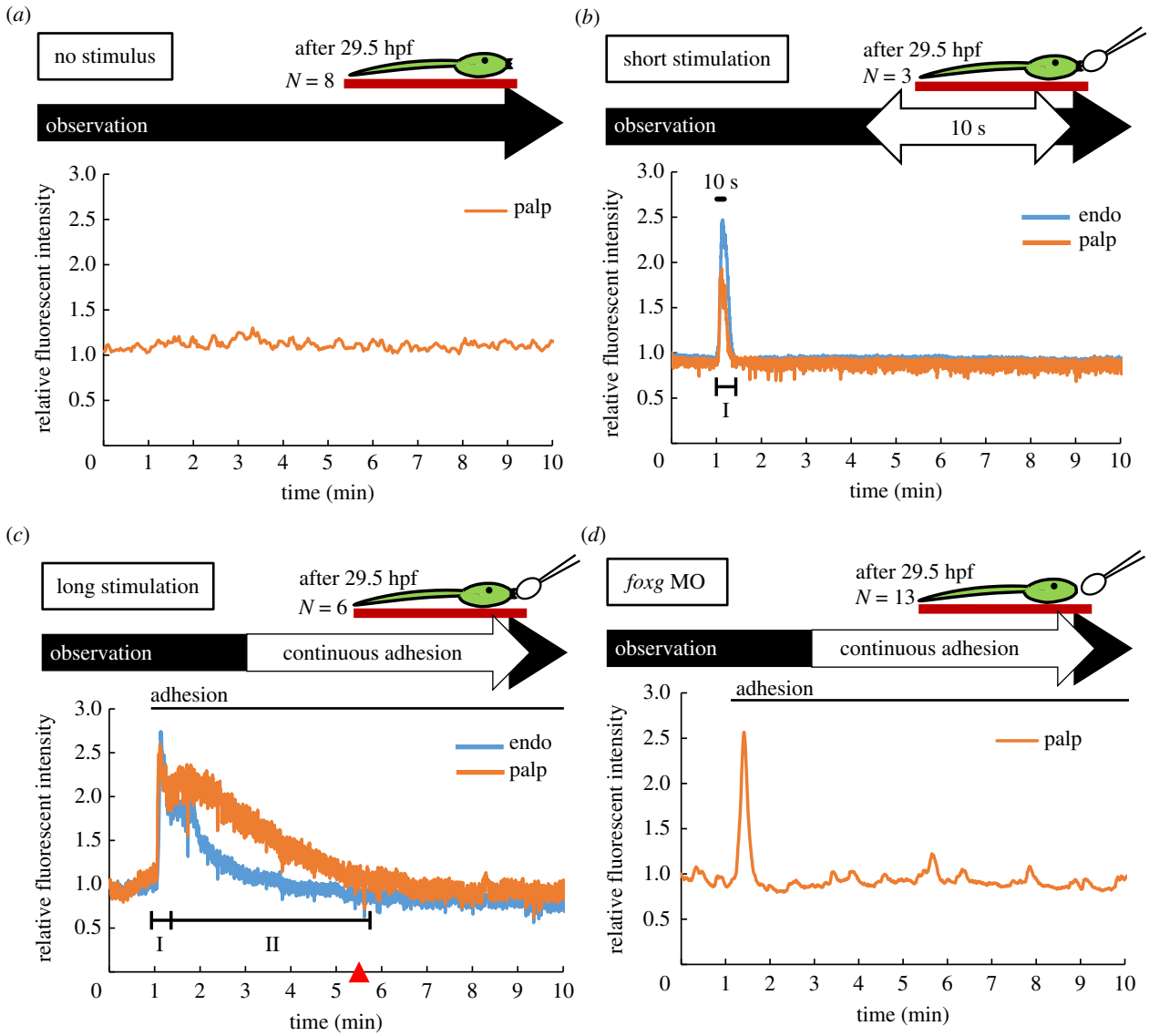

Figure 4. Comparison of Ca^{2+} dynamics in different lengths of mechanical stimulation. (*a*) Ca^{2+} dynamics in a swimming larva after 29.5 hpf in the absence of mechanical stimulation. The relative fluorescence intensity in palps (orange). Ca^{2+} activity stayed at basal level and no Ca^{2+} transients were observed in the palps. (*b*) Ca^{2+} dynamics in larva palps (orange) and posterior trunk region (blue) with short stimulus (10 s duration). The stimulation started at 1 min (black bar). Ca^{2+} transient in palps followed by trunk region similar to the Ca^{2+} transient in Phase I was observed. (*c*) Continuous mechanical stimulation induced a long-term transient in Phase II after Phase I. At the end of Phase II, tail regression was observed (red triangle). Stimulation began at 1 min (black bar). (*d*) Ca^{2+} dynamics in *Foxg* MO injected larva under continuous adhesion. Stimulation began at 1 min (black bar). (Online version in colour.)

Phase I was strongly coupled to mechanosensation (figure 3, figure 4 and table 1) and Phase II was coupled to tail regression (figure 4*c* and table 1). We considered that the two rounds of Ca^{2+} transients in these phases were essential for *Ciona* tail regression during metamorphosis. According to a previous study, at least 28 min of adhesion is necessary for tail regression, and individuals more than 29.5 hpf start tail regression after an average adhesion time of 32 min [28]. By contrast, five out of six larvae start tail regression less than 28 min after adhesion in our experiments. The average time between adhesion and tail regression was 12 ± 4.3 min. These different response times may be due to differences in the substrate or in the strength of adhesion.

Is there a causal connection between Phase I and Phase II? We consider there is a temporal threshold of Ca^{2+} in Phase I that is prerequisite for activation of Phase II. From our results, less than 10 s stimulation induced only Phase I whereas an average of 12 min continuous stimulation induced both Phase I and Phase II Ca^{2+} transients. In our experimental system, Phase II is only observed after Phase I occurs (table 1). Therefore, we think Phases I and II are tightly coupled also in the natural condition. However, inhibition of the specification of the papilla sensory neurons by *Foxg* MO decoupled them (figure 4*d*). Further studies of papillary sensory neurons will provide a better understanding of the mechanisms that will cause Phase II.

(a) Papillary cells activated by mechanical stimulation

Our results suggest that the papillae include mechanically sensitive sensory cells. There are three types of cells in the papillae, namely four axial columnar cells (ACC), four lateral primary sensory neurons (PNS), and 12 central collocytes (CC). Their nuclei are in posterior papillae processes and tissues that make up the anterior trunk [8]. The mechanism

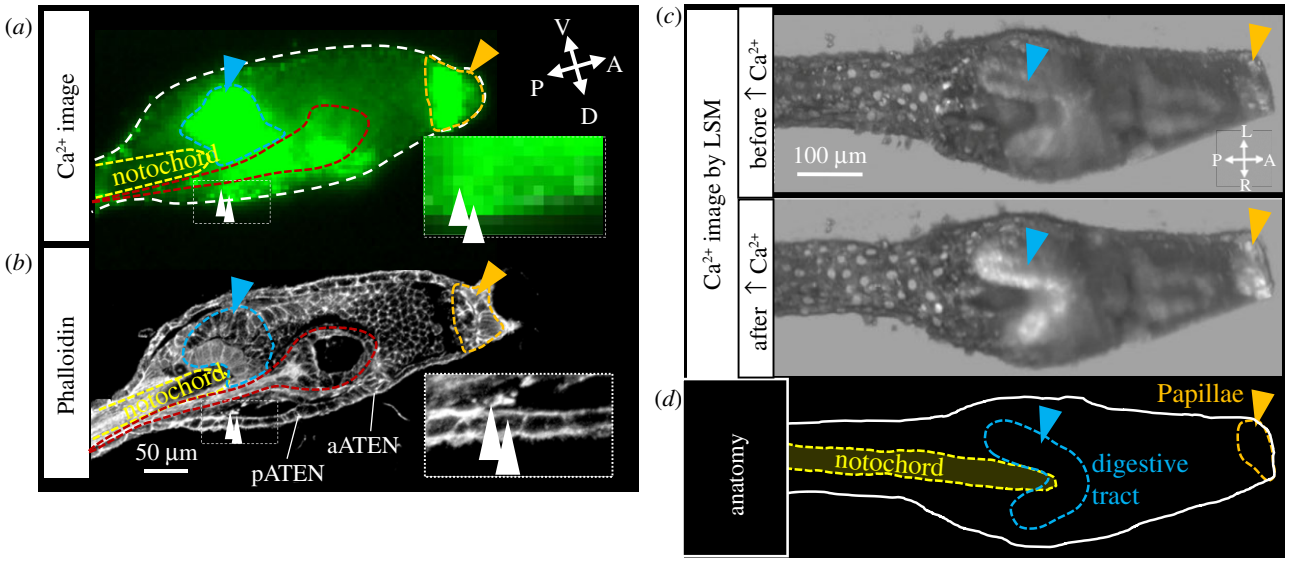

Figure 5. Identification of tissues expressing Ca^{2+} transient during Phase I. (*a*) Ca^{2+} image of figure 2*d*, time = 1 min 6 s. (*b*) CLSM image of a larval trunk by phalloidin staining in the same developmental stage of the larva in (*a*). pATEN: posterior apical trunk epidermal neuron, aATEN: anterior apical trunk epidermal neuron. (*c*) The transverse sectioned three-dimensional Ca^{2+} image of larval trunk before and after the Ca^{2+} transient in the palps by LSM. (*d*) The anatomical explanation of (*c*). In all figures, anatomically identical regions are indicated by the same colour e.g. palps (orange arrowheads or dotted line), digestive tract primordia (blue arrowheads or dotted lines), CNS (red dotted line), notochord (yellow dotted line), and dorsally localized cells in the posterior trunk (white arrowheads). Abbreviations: A, anterior; D, dorsal; L, left; P, posterior; R, right; V: ventral. (Online version in colour.)

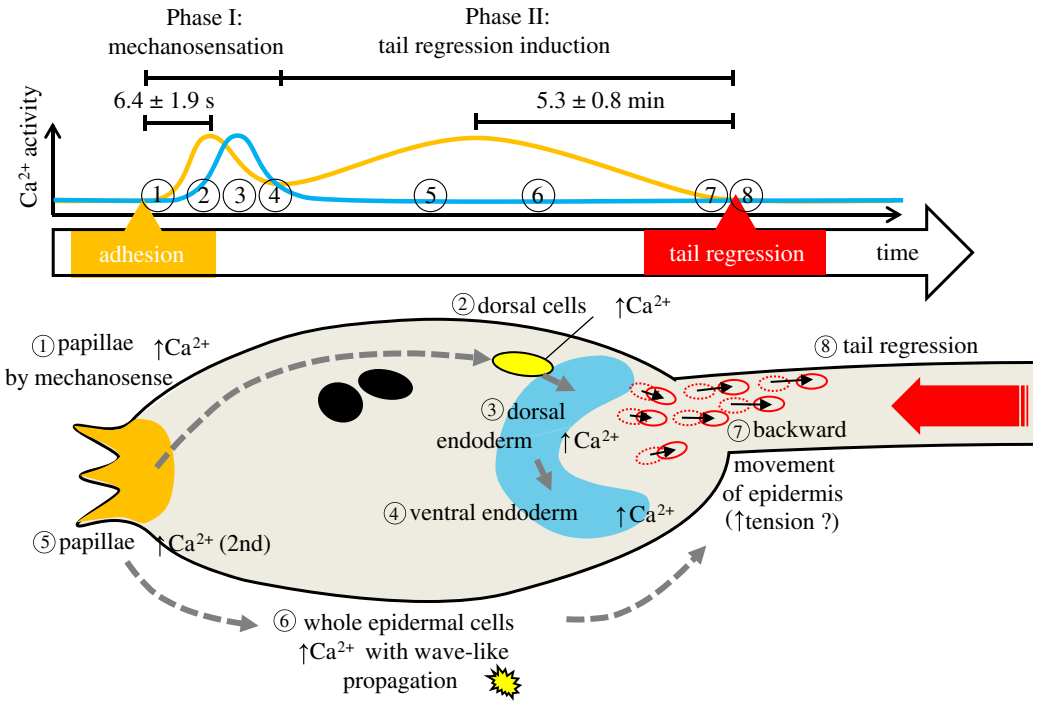

Figure 6. Observed Ca^{2+} transients from mechanical stimulation to tail regression. In Phase I, the order of Ca^{2+} transients observed in this study was as follows: (1) Papillary Ca^{2+} transient in response to mechanical stimuli. (2) Ca^{2+} transient in the dorsally localized cells immediately after (1). (3) The Ca^{2+} transient in the dorsal endoderm (presumptive digestive tract) near the dorsally localized cells. (4). Ca^{2+} transient in the dorsal endoderm propagated to the ventral endoderm. In Phase II, the observed Ca^{2+} dynamics were as follows: (5) The second round of Ca^{2+} transient in papillae. (6) Ca^{2+} increase in the entire epidermis with wave-like propagation. (7) The posterior trunk epidermis moves backward. Subsequently, (8) tail regression occurs. (Online version in colour.)

of metamorphosis signalling from papillae to other cells remains unsolved, but CCs and PNSs have been suggested to have exocytosis function [8]. This suggests that it may release signalling ligands via Ca^{2+}-dependent exocytosis.

We assumed that several ACCs, PNS, and CCs react to the mechanical stimulus. Although ACC and CC are not neurons, we need to determine whether they sense mechanical stimuli. Identifying the channels that control Ca^{2+} influx would help elucidate the underlying mechanism for mechanosensing by the papillae.

(b) Transmission of Ca^{2+} signals among different tissues during Phase I and Phase II

Our comprehensive Ca^{2+} imaging revealed the interplay of Ca^{2+} signalling in different tissues at the start of

metamorphosis. One of the surprising results in our study is the Ca^{2+} transient in endodermal cells surrounding the notochord in response to mechanical stimulation (figure 3*b*). Ca^{2+} transient has not been observed in the endoderm from gastrulation to the tailbud stage in previous studies [27]. Since this endodermal region differentiates into the digestive tract during metamorphosis, the Ca^{2+} transient in the endoderm may be related to the promotion of digestive tract differentiation. It is also interesting that dorsally localized cells in the posterior trunk responded during Phase I (figure 2 and figure 5, white arrowhead). The dorsally localized cells are located beneath the epidermis and close to the central nervous system (CNS). Although these cells are unknown, they do not appear to be identical to posterior apical trunk epidermal neuron (pATEN) nor anterior apical trunk epidermal neuron (aATEN) because the cells are more posterior (figure 5*b*).

During Phase II, wave-like Ca^{2+} propagations were observed in cells across the entire epidermis (figure 2*f*; electronic supplementary material, Video S3). This shows the direct evidence of metamorphic signals spread through epithelial conduction of Ca^{2+}. A similar epithelial-conduction model of metamorphic signal propagation has been proposed for the hydrozoan cnidarian *Mitrocomella polydiademata* [15]. Our method developed in this study can be applied to other species to test whether the Ca^{2+} transients that cause metamorphosis are evolutionarily conserved in other marine invertebrates.

Considering the backward movement of the epidermis that occurred following the Ca^{2+} propagations, these Ca^{2+} propagations might increase the tension within the entire epidermis to generate the pulling force required for tail regression. The tail epidermis has been proposed to generate a sufficiently strong force to absorb the axial organs into the trunk region [39] during tail regression. It was also confirmed that tail regression is inhibited by using cytochalasin B, indicating that actin fibres play an important role in tail regression [40]. Another hypothesis of the tail epidermis contraction to explain the tail regression during ascidian metamorphosis is based on apoptosis [21,41,42]. Krasovec *et al*. [41] reported that the tail regression depends on a postero-anterior wave of a caspase-dependent apoptosis coupled with a contraction event. This apoptosis wave might be triggered by the Phase II wave-like Ca^{2+} propagations in the epidermis.

Data accessibility. This article has no additional data.

Authors' contributions. M.K.W. carried out the experimental work, participated in data analysis, and drafted the manuscript; M.J.N. and S.S. collected LSM data and critically revised the manuscript; K.O. participated in the design of the study, coordinated the study, and critically revised the manuscript; K.H. conceived the study, designed the study, and wrote the manuscript. All authors gave final approval for publication and agree to be held accountable for the work performed therein.

Competing interests. We declare we have no competing interests.

Funding. This work was supported by JSPS KAKENHI grant nos. JP16H01451 and JP16K07426.

Acknowledgements. *Ciona intestinalis* type A (*Ciona robusta*) was provided by Dr. Yutaka Satou (Kyoto University) and Dr. Manabu Yoshida (University of Tokyo) with support from the National Bio-Resource Project of AMED, Japan. We express our appreciation to Dr. Yutaka Satou for providing MOs against Foxg. We thank Dr. Jean-Philippe Chambon for providing experimental protocols.

References

1. Essock-Burns T, Gohad NV, Orihuela B, Mount AS, Spillmann CM, Wahl KJ, Rittschof D. 2017 Barnacle biology before, during and after settlement and metamorphosis: a study of the interface. *J. Exp. Biol.* **220**, 194–207. (doi:10.1242/jeb.145094)
2. García-Lavandeira M, Silva A, Abad M, Pazos AJ, Sánchez JL, Pérez-Parallé ML. 2005 Effects of GABA and epinephrine on the settlement and metamorphosis of the larvae of four species of bivalve molluscs. *J. Exp. Mar. Bio. Ecol.* **316**, 149–156. (doi:10.1016/j.jembe.2004.10.011)
3. Ito S, Kawahara I, Hirayama I. 1994 Several inducers initiated settlement and metamorphosis Stichopus japonicus of Doliolaria Larvae of Sea Cucumber, Stichopus japonicus. *Suisan Zoshoku* **42**, 299–306. (doi:10.11233/aquaculturesci1953.42.299)
4. Jackson D, Leys SP, Hinman VF, Woods R, Lavin MF, Degnan BM. 2002 Ecological regulation of development: induction of marine invertebrate metamorphosis. *Int. J. Dev. Biol.* **46**, 679–686. (doi:10.1387/ijdb.12141457)
5. Kitamura H, Kitahara S, Koh HB. 1993 The induction of larval settlement and metamorphosis of two sea urchins, *Pseudocentrotus depressus* and *Anthocidaris crassispina*, by free fatty acids extracted from the coralline red alga *Corallina pilulifera*. *Mar. Biol.* **115**, 387–392. (doi:10.1007/BF00349836)
6. Hawes FB. 1958 Preliminary observations on the settlement of the actinula larva of the *Tubularia larynx* (Ellis & Solander). *Ann. Mag. Nat. Hist.* **1**, 147–155. (doi:10.1080/00222935 808650931)
7. Nakayama-Ishimura A, Chambon J, Horie T, Satoh N, Sasakura Y. 2009 Delineating metamorphic pathways in the ascidian *Ciona intestinalis*. *Dev. Biol.* **326**, 357–367. (doi:10.1016/j.ydbio.2008.11.026)
8. Zeng F, Wunderer J, Salvenmoser W, Hess MW, Ladurner P, Rothbächer U. 2019 Papillae revisited and the nature of the adhesive secreting collocytes. *Dev. Biol.* **448**, 183–198. (doi:10.1016/j.ydbio.2018.11.012)
9. Afsar A, De Nys R, Steinberg P. 2003 The effects of foul-release coatings on the settlement and behaviour of cyprid larvae of the barnacle Balanus amphitrite amphitrite Darwin. *Biofouling* **19**, 105–110. (doi:10.1080/0892701021000057909)
10. Hadfield M, Paul V. 2001 Natural Chemical Cues for Settlement and Metamorphosis of Marine-Invertebrate Larvae. In *Marine Chemical Ecology* (eds JB McClintock, BJ Baker), pp. 431–461. Boca Raton, FL: CRC Press.
11. Nellis P, Bourget E. 1996 Influence of physical and chemical factors on settlement and recruitment of the hydroid *Tubularia larynx*. *Mar. Ecol. Prog. Ser.* **140**, 123–139. (doi:10.3354/meps140123)
12. Hadfield M, Meleshkevitch E, Boudko D. 2000 The apical sensory organ of a gastropod veliger is a receptor for settlement cues. *Biol. Bull.* **198**, 67–76. (doi:10.2307/1542804)
13. Murabe N, Hatoyama H, Komatsu M, Kaneko H, Nakajima Y. 2007 Adhesive papillae on the brachiolar arms of brachiolaria larvae in two starfishes, *Asterina pectinifera* and *Asterias amurensis*, are sensors for metamorphic inducing factor(s). *Dev. Growth Differ.* **49**, 647–656. (doi:10.1111/j.1440-169X.2007.00959.x)
14. Leise EM, Kempf SC, Durham NR, Gifondorwa DJ. 2004 Induction of metamorphosis in the marine gastropod *Ilyanassa obsoleta*: 5HT, NO and Programmed Cell Death. *Acta Biol. Hung.* **55**, 293–300. (doi:10.1556/ABiol.55.2004.1-4.35)
15. Freeman G, Ridgway EB. 1990 Cellular and intracellular pathways mediating the metamorphic stimulus in hydrozoan planulae. *Roux's Arch. Dev. Biol.* **199**, 63–79. (doi:10.1007/BF02029553)
16. Freeman G. 1993 Metamorphosis in the Brachiopod Terebratalia : evidence for a role of calcium channel function and the dissociation of shell formation from settlement. *Biol. Bull.* **184**, 15–24. (doi:10.2307/1542376)

17. Clare AS. 1996 Signal transduction in barnacle settlement: calcium re-visited. *Biofouling* **10**, 141–159. (doi:10.1080/08927019609386276)
18. Biggers WJ, Laufer H. 1999 Settlement and metamorphosis of capitella larvae induced by juvenile hormone-active compounds is mediated by protein kinase C and ion channels. *Biol. Bull.* **196**, 187–198. (doi:10.2307/1542564)
19. Nakanishi N, Stoupin D, Degnan SM, Degnan BM. 2015 Sensory flask cells in sponge larvae regulate metamorphosis via calcium signaling. *Integr. Comp. Biol.* **55**, 1018–1027. (doi:10.1093/icb/icv014)
20. Pennati R, Rothbächer U. 2015 Bioadhesion in ascidians: a developmental and functional genomics perspective. *Interface Focus* **5**, 20140061. (doi:10.1098/rsfs.2014.0061)
21. Chambon J-PP, Soule J, Pomies P, Fort P, Sahuquet A, Alexandre D, Mangeat P-HH, Baghdiguian S. 2002 Tail regression in *Ciona intestinalis* (Prochordate) involves a Caspase-dependent apoptosis event associated with ERK activation. *Development* **129**, 3105–3114.
22. Liu B, Satou Y. 2019 Foxg specifies sensory neurons in the anterior neural plate border of the ascidian embryo. *Nat. Commun.* **10**, 1–10. (doi:10.1038/s41467-019-12839-6)
23. Imai JH, Meinertzhagen IA. 2007 Neurons of the ascidian larval nervous system in *Ciona intestinalis*: I. Central nervous system. *J. Comp. Neurol.* **501**, 316–334. (doi:10.1002/cne.21246)
24. Horie T, Kusakabe T, Tsuda M. 2008 Glutamatergic networks in the *Ciona intestinalis* larva. *J. Comp. Neurol.* **508**, 249–263. (doi:10.1002/cne.21678)
25. Torrence SA, Cloney RA. 1982 Nervous system of ascidian larvae: caudal primary sensory neurons. *Zoomorphology* **99**, 103–115. (doi:10.1007/BF00310303)
26. Karaiskou A, Swalla BJ, Sasakura Y, Chambon J-PP. 2015 Metamorphosis in solitary ascidians. *Genesis* **53**, 34–47. (doi:10.1002/dvg.22824)
27. Akahoshi T, Hotta K, Oka K. 2017 Characterization of calcium transients during early embryogenesis in ascidians *Ciona robusta* (*Ciona intestinalis* type A) and *Ciona savignyi*. *Dev. Biol.* **431**, 205–214. (doi:10.1016/j.ydbio.2017.09.019)
28. Matsunobu S, Sasakura Y. 2015 Time course for tail regression during metamorphosis of the ascidian *Ciona intestinalis*. *Dev. Biol.* **405**, 71–81. (doi:10.1016/j.ydbio.2015.06.016)
29. Hotta K, Dauga D, Manni L. 2020 The ontology of the anatomy and development of the solitary ascidian Ciona: the swimming larva and its metamorphosis. *Sci. Rep.* **10**, 17916. (doi:10.1038/s41598-020-73544-9)
30. Negishi T, Mcdougall A, Yasuo H. 2013 Practical tips for imaging ascidian embryos. *Dev. Growth Differ.* **55**, 446–453. (doi:10.1111/dgd.12059)
31. Hotta K, Mitsuhara K, Takahashi H, Inaba K, Oka K, Gojobori T, Ikeo K. 2007 A web-based interactive developmental table for the Ascidian *Ciona intestinalis*, including 3D real-image embryo reconstructions: I. From fertilized egg to hatching larva. *Dev. Dyn.* **236**, 1790–1805. (doi:10.1002/dvdy.21188)
32. Terakubo HQ, Nakajima Y, Sasakura Y, Horie T, Konno A, Takahashi H, Inaba K, Hotta K, Oka K. 2010 Network structure of projections extending from peripheral neurons in the tunic of ascidian larva. *Dev. Dyn.* **239**, 2278–2287. (doi:10.1002/dvdy.22361)
33. Yokoyama TD, Hotta K, Oka K. 2014 Comprehensive morphological analysis of individual peripheral neuron dendritic arbors in ascidian larvae using the photoconvertible protein kaede. *Dev. Dyn.* **243**, 1362–1373. (doi:10.1002/dvdy.24169)
34. Yoshida M, Sensui N, Inoue T, Morisawa M, Mikoshiba K. 1998 Role of two series of Ca^{2+} oscillations in activation of ascidian eggs. *Dev. Biol.* **203**, 122–133. (doi:10.1006/dbio.1998.9037)
35. Manni L, Pennati R. 2015 Tunicata. In *Structure and evolution of invertebrate nervous systems* (eds S-R Andreas, S Harzsch, G Purschke), pp. 699–718. Oxford, UK: Oxford University Press.
36. Ryan K, Lu Z, Meinertzhagen IA. 2017 The peripheral nervous system of the ascidian tadpole larva: types of neurons and their synaptic networks. *J. Comp. Neurol.* **526**, 583–608. (doi:10.1002/cne.24353)
37. Konno A, Kaizu M, Hotta K, Horie T, Sasakura Y, Ikeo K, Inaba K. 2010 Distribution and structural diversity of cilia in tadpole larvae of the ascidian *Ciona intestinalis*. *Dev. Biol.* **337**, 42–62. (doi:10.1016/j.ydbio.2009.10.012)
38. Nakazawa K, Yamazawa T, Moriyama Y, Ogura Y, Kawai N, Sasakura Y, Saiga H. 2013 Formation of the digestive tract in *Ciona intestinalis* includes two distinct morphogenic processes between its anterior and posterior parts. *Dev. Dyn.* **242**, 1172–1183. (doi:10.1002/dvdy.24009)
39. Numakunai T. 1977 Hentai. In *Gendai doubutsugaku No kadai,* vol. 5 (ed. TZS of Japan), pp. 135–175. Tokyo, Japan: Gakkai Shuppan Center.
40. Lash JW, Cloney RA, Minor RR. 1973 The effect of cytochalasin b upon tail resorption and metamorphosis in ten species of. *Biol. Bull.* **145**, 360–372. (doi:10.2307/1540046)
41. Krasovec G, Robine K, Quéinnec E, Karaiskou A, Chambon JP. 2019 Ci-hox12 tail gradient precedes and participates in the control of the apoptotic-dependent tail regression during Ciona larva metamorphosis. *Dev. Biol.* **448**, 237–246. (doi:10.1016/j.ydbio.2018.12.010)
42. Chambon J-P, Nakayama A, Takamura K, McDougall A, Satoh N. 2007 ERK- and JNK-signalling regulate gene networks that stimulate metamorphosis and apoptosis in tail tissues of ascidian tadpoles. *Development* **134**, 1203–1219. (doi:10.1242/dev.002220)